6534 *Inorg. Chem.* **2009**, *48*, 6534–6547
DOI: 10.1021/ic900469y

Inorganic Chemistry
Article

Organometallic Complexes for Nonlinear Optics. 42.[1] Syntheses, Linear, and Nonlinear Optical Properties of Ligated Metal-Functionalized Oligo(*p*-phenyleneethynylene)s

Gulliver T. Dalton,[†,‡] Marie P. Cifuentes,[†] Laurance A. Watson,[†] Simon Petrie,[†] Robert Stranger,[†] Marek Samoc,*[,‡,§] and Mark G. Humphrey*[,†]

[†]*Research School of Chemistry and* [‡]*Laser Physics Centre, Research School of Physics and Engineering, Australian National University, Canberra ACT 0200, Australia, and* [§]*Institute of Physical and Theoretical Chemistry, Wroclaw University of Technology, 50-370 Wroclaw, Poland*

Received March 9, 2009

A combination of UV−vis−NIR spectroscopy, femtosecond Z-scan measurements, and time-dependent density functional theory (TD-DFT) calculations have been used to comprehensively investigate the linear optical and nonlinear optical (NLO) properties of π-delocalizable metal-functionalized oligo(phenyleneethynylene)s. A range of unsymmetrically or symmetrically end-functionalized mono-, di-, tri-, penta-, hepta-, and nona(phenyleneethynylene)s were synthesized, with larger examples bearing varying numbers of 2,5-di(hexyloxy)phenyl groups to ensure sufficient solubility of the metal complex derivatives. The effect of incorporating varying numbers of solubilizing substituents in the OPE bridge, peripheral group modification, OPE lengthening, coligand variation, and metal location in the OPE on the linear optical properties has been established, with the first three molecular modifications resulting in significant changes in the optical absorption maxima. TD-DFT calculations reveal that the most intense transition in the linear optical spectra is localized on the OPE bridge and involves excitation from acetylenic to cumulenic molecular orbitals that are not greatly spatially separated from one another. The nonlinear optical properties are dominated by two-photon absorption, which for all but 1,4-{*trans*-[RuCl(dppm)$_2$]C≡C}$_2$C$_6$H$_4$ appears as a band around 11400 cm^{-1} and a sharp increase of nonlinear absorption at frequencies >17000 cm^{-1}. Surprisingly, there is relatively little influence of the length of the OPE bridge on the magnitude of the two-photon absorption cross sections, which are in the range 300−1000 GM.

Introduction

Oligo(*p*-phenyleneethynylene)s (OPEs) have been of considerable interest in recent years for a number of reasons. For example, their linear conjugated structure affords useful molecular building blocks,[2−5] and their solid-state photophysical properties[6−9] and solution nonlinear optical (NLO) properties have attracted attention.[10−15] Introduction of ligated metal units into an OPE structure can add a new dimension: the resultant transition metal OPE complexes can potentially possess a number of useful properties such as luminescence, reversible redox chemistry, and accessible

*To whom correspondence should be addressed. E-mail: mark.humphrey@anu.edu.au (M.G.H.), marek.samoc@pwr.wroc.pl (M.S.). Phone: +61 2 6125 2927 (M.G.H.), +48 71 320 44 66 (M.S.). Fax: +61 2 6125 0760 (M.G.H.), +48 71 320 33 64 (M.S.).

(1) Part 41: Fondum, T. N.; Green, K. A.; Randles, M. D.; Cifuentes, M. P.; Willis, A. C.; Teshome, A.; Asselberghs, I.; Clays, K.; Humphrey, M. G. *J. Organomet. Chem.* **2008**, *693*, 1605.
(2) Müllen, K.; Wegner, G. *Electronic Materials: The Oligomer Approach*; Wiley-VCH: Weinheim, 1998.
(3) Dhirani, A.; Zehner, R.; Hsung, R.; Guyot-Sionnest, P.; Sita, L. R. *J. Am. Chem. Soc.* **1996**, *118*, 3319.
(4) Andres, R. P.; Bielefeld, J. D.; Henderson, J. I.; Janes, D. B.; Kolagunta, V. R.; Kubiak, C. P.; Mahoney, W. J. *Science* **1996**, *273*, 1690.
(5) For a review on molecular wires, see: James, D. K.; Tour, J. M. *Top. Curr. Chem.* **2005**, *257*, 33.
(6) See, for example: Yang, J.-S.; Yan, J.-L.; Hwang, C.-Y.; Chiou, S.-Y.; Liau, K.-L.; Tsai, H.-H. G.; Lee, G.-H.; Peng, S.-M. *J. Am. Chem. Soc.* **2006**, *128*, 14109, and references therein.
(7) Zhou, N.; Wang, L.; Thompson, D. W.; Zhao, Y. *Tetrahedron Lett.* **2007**, *48*, 3563.
(8) Yamaguchi, Y.; Ochi, T.; Wakamiya, T.; Matsubara, Y.; Yoshida, Z.-i. *Org. Lett.* **2006**, *8*, 717.
(9) James, P. V.; Sudeep, P. K.; Suresh, C. H.; George Thomas, G. *J. Phys. Chem. A* **2006**, *110*, 4329.
(10) Meier, H.; Ickenroth, D.; Stalmach, U.; Koynov, K.; Bahtiar, A.; Bubeck, C. *Eur. J. Org. Chem.* **2001**, 3643.
(11) Wautelet, P.; Moroni, M.; Oswald, L.; Moigne, J. L.; Pham, A.; Bigot, J.-Y. *Macromolecules* **1996**, *29*, 446.
(12) Koynov, K.; Bahtiar, A.; Bubeck, C.; Mühling, B.; Meier, H. *J. Phys. Chem. B* **2005**, *109*, 10184.
(13) Zhao, Y.; Shirai, Y.; Slepkov, A. D.; Cheng, L.; Alemany, L. B.; Sasaki, T.; Hegman, F. A.; Tour, J. M. *Chem.—Eur. J.* **2005**, *11*, 3643.
(14) Cheng, L.-T.; Tam, W.; Stevenson, S. H.; Meredith, G. R. *J. Phys. Chem.* **1991**, *95*, 10631.
(15) Cheng, L.-T.; Tam, W.; Marder, S. R.; Steigman, A. E.; Rikken, G.; Spangler, C. W. *J. Phys. Chem.* **1991**, *95*, 10643.

Published on Web 06/23/2009
© 2009 American Chemical Society

mixed valence states, and such complexes have been examined for molecular electronics and liquid crystal applications.[16,17] Despite this interest, the physical properties of well-defined series of systematically varied metal-terminated OPEs are yet to be explored; although there have been a large number of reports of ligated-metal-capped 1,4-diethynylarenes (**A**, Chart 1),[18−53] and their corresponding polymers (in which the ligated metals are in the repeat units: **B**, Chart 1),[43−49,51−66] there are considerably fewer reports of well-characterized "dimers" (**C**, Chart 1)[50−52,64,67−71] or well-defined higher oligomers. Noteworthy series of the latter include (PhC≡C){Pt(PBu$^n_3$)$_2$(C≡C-4-C$_6$H$_4$C≡C)}$_n$Pt(PBu$^n_3$)$_2$(C≡CPh) (n = 1−4, 6) from Schanze and co-workers[72,73] and HC≡C-2,5-(C$_{12}$H$_{25}$)$_2$C$_6$H$_2$C≡C{Pt$_6$(μ-PBu$^t_2$)$_4$(CO)$_4$(C≡C-2,5-(C$_{12}$H$_{25}$)$_2$C$_6$H$_2$C≡C)}$_n$ {Pt$_6$(μ-PBu$^t_2$)$_4$(CO)$_4$(C≡C-2,5-(C$_{12}$H$_{25}$)$_2$C$_6$H$_2$-C≡CH)}$_n$ (n = 2, 4, many) from Leoni et al.[74]

Excluding the "monomer" case (**A**, Chart 1), the literature for metal termination of OPEs is sparse, specific examples being (triphenylphosphine)gold and cluster-capped tri(phenyleneethynylene)[75] (**D**, Chart 1) and platinum-tri(aryleneethynylene) polymers (**E**, Chart 1).[76] Che and co-workers

(16) Klein, A.; Lavastre, O.; Fiedler, J. *Organometallics* **2006**, *25*, 635.
(17) Bongsoo, K.; Beebe, J. M.; Olivier, C.; Rigaut, S.; Touchard, D.; Kushmerick, J. G.; Zhu, X.-Y.; Frisbie, C. D. *J. Phys. Chem. C* **2007**, *111*, 7521, and references therein.
(18) Yam, V. W.-W.; Fung, W. K.-M.; Cheung, K.-K. *Chem. Commun.* **1997**, 963.
(19) Samoc, M.; Gauthier, N.; Cifuentes, M. P.; Paul, F.; Lapinte, C.; Humphrey, M. G. *Angew. Chem., Int. Ed.* **2006**, *45*, 7376.
(20) Albertin, G.; Agnoletto, P.; Antoniutti, S. *Polyhedron* **2002**, *21*, 1755.
(21) Wong, K. M.-C.; Lam, K. C.-F.; Ko, C.-C.; Zhu, N.; Yam, V. W.-W.; Roué, S.; Lapinte, C.; Fathallah, S.; Costuas, K.; Kahlal, S.; Halet, J.-F. *Inorg. Chem.* **2003**, *42*, 7086.
(22) Khan, M. S.; Al-Suti, M. K.; Mahon, M. F.; Male, L.; Raithby, P. R. *Acta Crystallogr.* **2003**, *E59*, m833.
(23) Gao, L.-B.; Zhang, L.-Y.; Shi, L.-X.; Chaen, Z.-N. *Organometallics* **2005**, *24*, 1678.
(24) Khan, M. S.; Al-Suti, M. K.; Al-Mandhary, M. R. A.; Ahrens, B.; Bjernemose, J. K.; Mahon, M. F.; Male, L.; Raithby, P. R.; Friend, R. H.; Köhler, A.; Wilson, J. S. *Dalton Trans.* **2003**, 65.
(25) Ghazala, S. I.; Paul, F.; Toupet, L.; Roisnel, T.; Hapiot, P.; Lapinte, C. *J. Am. Chem. Soc.* **2006**, *128*, 2463.
(26) Medei, L.; Orian, L.; Semeikin, O. V.; Peterleitner, M. G.; Ustynyuk, N. A.; Santi, S.; Durante, C.; Ricci, A.; Lo Sterzo, C. *Eur. J. Inorg. Chem.* **2006**, 2582.
(27) Weyland, T.; Ledoux, I.; Brasselet, S.; Zyss, J.; Lapinte, C. *Organometallics* **2000**, *19*, 5235.
(28) Ara, I.; Berengure, J. R.; Eguiz-Eabal, E.; Forniés, J.; Gómez, J.; Lalinde, E.; Sáez-Rocher, J. M. *Organometallics* **2000**, *19*, 4385.
(29) Albertin, G.; Antoniutti, S.; Bordignon, E.; Granzotto, M. *J. Organomet. Chem.* **1999**, *585*, 83.
(30) Bruce, M. I.; Hall, B. C.; Low, P. J.; Skelton, B. W.; White, A. H. *J. Organomet. Chem.* **1999**, *592*, 74.
(31) Younus, M.; Long, N. J.; Raithby, P. R.; Lewis, J. *J. Organomet. Chem.* **1998**, *570*, 55.
(32) Colbert, M. C. B.; Lewis, J.; Long, N. J.; Raithby, P. R.; Younus, M.; White, A. J. P.; Williams, D. J.; Payne, N. N.; Yellowlees, L.; Beljonne, D.; Chawdhury, N.; Friend, R. H. *Organometallics* **1998**, *17*, 3034.
(33) Irwin, M. J.; Vittal, J. J.; Puddephatt, R. J. *Organometallics* **1997**, *16*, 3541.
(34) Beljonne, D.; Colbert, M. C. B.; Raithby, P. R.; Friend, R. H.; Brédas, J. L. *Synth. Met.* **1996**, *81*, 179.
(35) Hurst, S. K.; Cifuentes, M. P.; McDonagh, A. M.; Humphrey, M. G.; Samoc, M.; Luther-Davies, B.; Asselberghs, I.; Persoons, A. *J. Organomet. Chem.* **2002**, *642*, 259.
(36) Tykwinski, R. R.; Stang, P. J. *Organometallics* **1994**, *13*, 3203.
(37) Le Narvor, N.; Lapinte, C. *Organometallics* **1995**, *14*, 634.
(38) Jia, G.; Puddephatt, R. J.; Scott, J. D.; Vittal, J. J. *Organometallics* **1993**, *12*, 3565.
(39) Field, L. D.; George, A. V.; Laschi, F.; Malouf, E. Y.; Zanello, P. *J. Organomet. Chem.* **1992**, *435*, 347.
(40) Nast, R.; Moritz, J. *J. Organomet. Chem.* **1976**, *117*, 81.
(41) Nast, R.; Beyer, A. *J. Organomet. Chem.* **1980**, *194*, 125.
(42) Stang, P. J.; Tykwinski, R. R. *J. Am. Chem. Soc.* **1992**, *114*, 4411.
(43) Köhler, A.; Wilson, J. S.; Friend, R. H.; Al-Suti, M. K.; Khan, M. S.; Gerhard, A.; Bässler, H. *J. Chem. Phys.* **2002**, *116*, 9457.
(44) Vicente, J.; Chicote, M. T.; Alvarez-Falcón, M. M.; Abrisqueta, M. D.; Hernández, F. J.; Jones, P. G. *Inorg. Chim. Acta* **2003**, *347*, 67.
(45) Khan, M. S.; Al-Mandhary, M. R. A.; Al-Suti, M. K.; Al-Battashi, F. R.; Al-Saadi, S.; Ahrens, B.; Bjernemose, J. K.; Mahon, M. F.; Raithby, P. R.; Younus, M.; Chawdhury, N.; Köhler, A.; Marseglia, E. A.; Tedesco, E.; Feeder, N.; Teat, S. J. *Dalton Trans.* **2004**, 2377.
(46) Faulkner, C. W.; Ingham, S. L.; Khan, M. S.; Lewis, J.; Long, N. J.; Raithby, P. R. *J. Organomet. Chem.* **1994**, *482*, 139.
(47) Khan, M. S.; Kakkar, A. K.; Ingham, S. L.; Raithby, P. R.; Lewis, J.; Spencer, B.; Wittmann, F.; Friend, R. H. *J. Organomet. Chem.* **1994**, *472*, 247.
(48) Khan, M. S.; Davies, S. J.; Kakkar, A. K.; Schwartz, D.; Lin, B.; Johnson, B. F. G.; Lewis, J. *J. Organomet. Chem.* **1992**, *424*, 87.
(49) Fyfe, H. B.; Mlekuz, M.; Zargarian, D.; Taylor, N. J.; Marder, T. B. *J. Chem. Soc., Chem. Commun.* **1991**, 188.
(50) Kim, B.; Beebe, J. M.; Olivier, C.; Rigaut, S.; Touchard, D.; Kushmerick, J. G.; Zhu, X.-Y.; Frisbie, C. D. *J. Phys. Chem. C* **2007**, *111*, 7521.
(51) Wilson, J. S.; Köhler, A.; Friend, R. H.; Al-Suti, M. K.; Al-Mandhary, M. R. A.; Khan, M. S.; Raithby, P. R. *J. Chem. Phys.* **2000**, *113*, 7627.
(52) Long, N. J.; Wong, C. K.; White, A. J. P. *Organometallics* **2006**, *25*, 2525.
(53) La Groia, A.; Ricci, A.; Bassetti, M.; Masi, D.; Bianchini, C.; Lo Sterzo, C. *J. Organomet. Chem.* **2003**, *683*, 406.
(54) Fratoddi, I.; Altamura, P.; Lo Sterzo, C.; Furlani, A.; Galassi, E.; D'Amico, A.; Russo, M. V. *Polym. Adv. Technol.* **2002**, *13*, 269.
(55) Long, N. J.; White, A. J. P.; Williams, D. J.; Younus, M. *J. Organomet. Chem.* **2002**, *649*, 94.
(56) Fratoddi, I.; Battocchio, C.; Furlani, A.; Mataloni, P.; Polzonetti, G.; Russo, M. V. *J. Organomet. Chem.* **2003**, *674*, 10.
(57) Khan, M. S.; Al-Mandhary, M. R. A.; Al-Suti, M. K.; Corcoran, T. C.; Al-Mahrooqi, Y.; Attfield, J. P.; Feeder, N.; David, W. I. F.; Shankland, K.; Friend, R. H.; Köhler, A.; Marseglia, E. A.; Tedesco, E.; Tang, C. C.; Raithby, P. R.; Collings, J. C.; Roscoe, K. P.; Batsanov, A. S.; Stimson, L. M.; Marder, T. B. *New J. Chem.* **2003**, *27*, 140.
(58) Vicente, J.; Chicote, M. T.; Alvarez-Falcón, M. M.; Jones, P. G. *Organometallics* **2005**, *24*, 5956.
(59) Davies, S. J.; Johnson, B. F. G.; Khan, M. S.; Lewis, J. *J. Chem. Soc., Chem. Commun.* **1991**, 187.
(60) Lewis, J.; Khan, M. S.; Kakkar, A. K.; Johnson, B. F. G.; Marder, T. B.; Fyfe, H. B.; Wittmann, F.; Friend, R. H.; Dray, A. E. *J. Organomet. Chem.* **1992**, *425*, 165.
(61) Atherton, Z.; Faulkner, C. W.; Ingham, S. L.; Kakkar, A. K.; Khan, M. S.; Lewis, J.; Long, N. J.; Raithby, P. R. *J. Organomet. Chem.* **1993**, *462*, 265.
(62) Johnson, B. F. G.; Kakkar, A. K.; Khan, M. S.; Lewis, J. *J. Organomet. Chem.* **1991**, *409*, C12.
(63) Markwell, R. D.; Butler, I. S.; Kakkar, A. K.; Khan, M. S.; Al-Zakwani, Z. H.; Lewis, J. *Organometallics* **1996**, *15*, 2331.
(64) Vicente, J.; Chicote, M. T.; Alvarez-Falcón, M. M.; Jones, P. G. *Organometallics* **2005**, *24*, 2764.
(65) Wittmann, H. F.; Fuhrmann, K.; Friend, R. H.; Khan, M. S.; Lewis, J. *Synth. Met.* **1993**, *55*, 56.
(66) Irwin, M. J.; Jia, G.; Vittal, J. J.; Puddephatt, R. J. *Organometallics* **1996**, *15*, 5321.
(67) Leoni, P.; Marchetti, F.; Marchetti, L.; Pasquali, M. *Chem. Commun.* **2003**, 2372.
(68) Yam, V. W.-W.; Lo, W.-Y.; Lam, C.-H.; Fung, W. K.-M.; Wong, K. M.-C.; Lau, V. C.-Y.; Zhu, N. *Coord. Chem. Rev.* **2003**, *245*, 39.
(69) Yam, V. W.-W.; Fung, W. K.-M.; Wong, K. M.-C.; Lau, V. C.-Y.; Cheung, K.-K. *Chem. Commun.* **1998**, 777.
(70) Huang, C.-C.; Lin, Y.-C.; Lin, P.-Y.; Chen, Y.-J. *Eur. J. Org. Chem.* **2006**, 4510.
(71) Olivier, C.; Kim, B.; Touchard, D.; Rigaut, S. *Organometallics* **2008**, *27*, 509.
(72) Glusac, K.; Köse, M. E.; Jiang, H.; Schanze, K. S. *J. Phys. Chem., B* **2007**, *111*, 929.
(73) Liu, Y.; Jiang, S.; Glusac, K.; Powell, D. H.; Anderson, D. F.; Schanze, K. S. *J. Am. Chem. Soc.* **2002**, *124*, 12412.
(74) Leoni, P.; Marchetti, L.; Mohapatra, S. K.; Ruggeri, G.; Ricci, L. *Organometallics* **2006**, *25*, 4226.
(75) Khairul, W. M.; Porrès, L.; Albesa-Jové, D.; Senn, M. S.; Jones, M.; Lydon, D. P.; Howard, J. A. K.; Beeby, A.; Marder, T. B.; Low, P. J. *J. Cluster Sci.* **2005**, *17*, 65.
(76) Khan, M. S.; Kakkar, A. K.; Long, N. J.; Lewis, J.; Raithby, P. R.; Nguyen, P.; Marder, T. B.; Wittmann, F.; Friend, R. H. *J. Mater. Chem.* **1994**, *4*, 1227.

Chart 1[a]

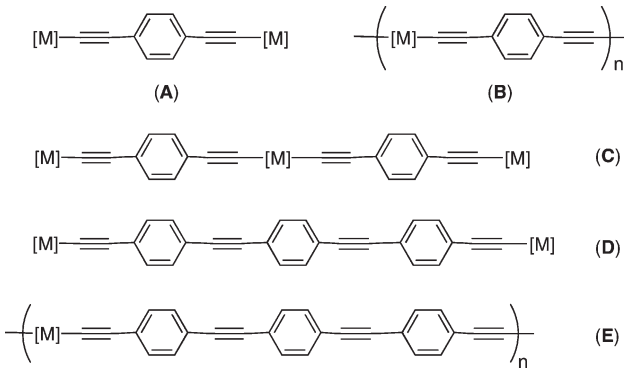

[a] [M] = ligated metal or cluster units.

have reported the photophysical properties of $(PCy_3)Au(C{\equiv}C\text{-}4\text{-}C_6H_4)_nC{\equiv}CAu(PCy_3)$ (n = 1−4),[77] and, particularly relevant to the present study, Klein et al. have summarized the evolution of cyclic voltammetric, UV−vis−NIR spectroelectrochemical, IR spectroelectrochemical, and EPR data for OPE chain-lengthening from monomer to trimer in the series $(dppe)_2ClRu(C{\equiv}C\text{-}4\text{-}C_6H_4)_nC{\equiv}CRu(dppe)_2$ (n = 1−3).[16] With these notable exceptions, physical properties studies of metal-containing OPEs are lacking.

We report herein syntheses of an extensive series of metal-terminated OPEs (up to a nona(phenyleneethynylene)), as well as routes to examples corresponding to differing metal sites in the OPE chain, the evolution of linear optical properties in metal-containing OPEs upon chain lengthening and metal site variation, rationalization of the optical spectra by time-dependent density functional theory (TD-DFT) studies, and a wavelength-dependence study of the cubic NLO properties of selected metal-containing OPEs by fs Z-scan measurements.

Experimental Section

General Conditions and Reagents. All reactions were performed under a nitrogen atmosphere with the use of standard Schlenk techniques unless otherwise stated. Solvents and reagents were obtained from commercial sources and used as received, unless otherwise indicated. CH_2Cl_2 was dried by distilling over calcium hydride, and NEt_3 was deoxygenated prior to use. Petrol refers to a fraction of petroleum with a boiling range 60−80 °C. Chromatography was on silica gel (230−400 mesh ASTM) or ungraded basic alumina. The following were prepared by literature procedures: $4\text{-}O_2NC_6H_4C{\equiv}CH$,[78] *cis*-$[RuCl_2(dppe)_2]$,[79] *cis*-$[RuCl_2(dppm)_2]$,[79] *trans*-$[Ru(4\text{-}C{\equiv}CC_6H_4NO_2)Cl(dppe)_2]$,[80] $4\text{-}PhC{\equiv}CC_6H_4C{\equiv}CH$,[81] $HC{\equiv}CC_6H_4\text{-}4\text{-}C{\equiv}CC_6H_4\text{-}4\text{-}C{\equiv}CH$,[82] 2,5-[5-$HC{\equiv}C$-1,4-$\{Me(CH_2)_5O\}_2C_6H_2$-2-$C{\equiv}C]_2$-1,4-$\{Me(CH_2)_5O\}_2C_6H_2$,[83] 1,4-{*trans*-$[RuCl(dppm)_2]C{\equiv}C\}_2C_6H_4$ (**31**).[46] The synthesis of *trans*-$[RuCl(dppe)_2](C{\equiv}C\text{-}4\text{-}C_6H_4)_3C{\equiv}C$-*trans*-$[RuCl(dppe)_2]$ (**30**) was reported during the course of this work.[16] The syntheses of **1**-**17** are described in the Supporting Information.

Instrumentation. Electrospray ionization (ESI) (both unit resolution and HR) mass spectra were recorded using a Bruker Apex 4.7T FTICR-MS at the Australian National University. Fast atom bombardment (FAB) mass spectra (30 kV Ar, 1 mA, accelerating potential 8 kV, 3-nitrobenzyl alcohol matrix) were recorded using an Autospec instrument at the University of Western Australia or a Micromass Zabspec instrument at the Institut für Organische Chemie, Universität Erlangen-Nürnberg. All mass spectra peaks are reported as m/z (assignment, relative intensity). Microanalyses were carried out at the Australian National University. Infrared spectra were recorded as CH_2Cl_2 (unless stated otherwise) solutions using a Perkin-Elmer System 2000 FT-IR. ^1H and ^{31}P NMR spectra were recorded using a Varian Gemini-300 FT NMR spectrometer and residual chloroform (7.24 ppm) or external 85% H_3PO_4 (0.0 ppm) as reference, respectively. ^{31}P NMR spectra were recorded with a small amount of NEt_3 added to ensure all sample was in the alkynyl rather than the vinylidene form. UV−vis−NIR transmission spectra were recorded in CH_2Cl_2 (unless stated otherwise) in 1 cm quartz cells using a Cary 5 spectrophotometer and are reported as λ_{max} nm (ε M^{-1} cm^{-1}).

Synthesis of Alkynylruthenium Complexes. *trans,trans*-$[(dppm)_2ClRu(C{\equiv}C\text{-}4\text{-}C_6H_4C{\equiv}C\text{-}4\text{-}C_6H_4C{\equiv}C)RuCl(dppm)_2]$ (18). $NaPF_6$ (71 mg, 0.42 mmol) was added to a solution of $(4\text{-}HC{\equiv}CC_6H_4)_2C{\equiv}C$ (30 mg, 0.13 mmol) and *cis*-$[RuCl_2(dppm)_2]$ (311 mg, 0.33 mmol) in CH_2Cl_2 (30 mL), and the mixture heated at reflux for 16 h. NEt_3 (10 mL) was added on cooling, and the mixture was placed on a small basic alumina column and eluted with CH_2Cl_2. The eluate was taken to dryness and triturated with ether to give a light yellow solid (**18**, 118 mg, 44%). Anal. Calcd for $C_{118}H_{96}Cl_2P_8Ru_2$ C 69.65, H 4.75; found: C 69.54, H 4.90%. ^1H NMR: δ 7.49−6.98 (m, 88H, Ph + C_6H_4), 4.89 (m, 8H, PCH_2P). ^{31}P NMR: δ −5.9. IR: 2068 $\nu(C{\equiv}C)$ cm^{-1}. ESI MS: 2035 ($[M]^+$, 7), 1999 ($[M-Cl]^+$, 6), 1130 ($[M-Ru(dppm)_2Cl]^+$, 7), 869 ($[Ru(dppm)_2]^+$, 100). UV−vis−NIR (THF): 401 (28400). The syntheses of **19**−**29** are similar and are reported in the Supporting Information.

Theoretical Methods. Density functional theory (DFT) calculations were executed in this study using the Amsterdam Density Functional (ADF) program, version ADF 2006.01,[84] developed by Baerends et al.[85,86] Calculations were performed in parallel mode on the AlphaServer supercomputer housed at the ANU Supercomputer Facility and operated under the Australian Partnership for Advanced Computing.

Calculations in C_{2v} or D_{2d} symmetry were pursued on a large range of models. Here we employ the notation *i*M*j*M*k* to represent a structure in which M is a *trans*-$(PH_2CH_2PH_2)_2Ru$ moiety and *i*, *j*, and *k* are integers showing the number of phenylethynyl links (or, in the case of *j*, the length of the ethynyl(phenylethynyl)$_j$ chain) in each portion of the complex. The structures categorized here include 0M*j*M0 (j = 1, 2, 3, 5, 7, 9), 1M*j*M1 (j = 1, 3, 5, 7), 2M*j*M2 (j = 1, 3, 5), 3M*j*M3 (j = 1, 3), and 4M1M4, with the i = 0 and k = 0 examples being chloride-terminated. In addition, di- and/or hexa-methoxylated structures have been characterized for 0M*j*M0 (j = 3, 5, 7, 9), 1M3M1, and 2M*j*M2 (j = 3, 5).

In all calculations and for all atoms, the Slater type orbital basis sets used were of triple-ζ-plus-polarization

(77) Chao, H.-Y.; Lu, W.; Li, Y.; Chan, M. C. W.; Che, C.-M.; Cheung, K.-K.; Zhu, N. *J. Am. Chem. Soc.* **2002**, *124*, 14696.
(78) Takahashi, S.; Kuroyama, Y.; Sonogashira, K.; Hagihara, N. *Synthesis* **1980**, 627.
(79) Chaudret, B.; Commenges, G.; Poilblanc, R. *J. Chem. Soc., Dalton Trans.* **1984**, 1635.
(80) Touchard, D.; Haquette, P.; Guesmi, S.; Pichon, L. L.; Daridor, A.; Toupet, L.; Dixneuf, P. H. *Organometallics* **1997**, *16*, 3640.
(81) Lavastre, O.; Cabioch, S.; Dixneuf, P. H.; Vohlidal, J. *Tetrahedron* **1997**, *53*, 7595.
(82) Simpson, C. D.; Brand, J. D.; Berresheim, A. J.; Przybilla, L.; Räder, H. J.; Müllen, K. *Chem.—Eur. J.* **2002**, *8*, 1424.
(83) Zhou, C.-Z.; Liu, T.; Xu, J.-M.; Chen, Z.-K. *Macromolecules* **2003**, *36*, 1457.
(84) Baerends, E. J. et al. S.C.M., Theoretical Chemistry, Vrije Universiteit: Amsterdam, The Netherlands, 2004; http://www.scm.com (accessed 2006).
(85) Fonseca Guerra, C. F.; Snijders, J. G.; te Velde, G.; Baerends, E. J. *Theor. Chem. Acc.* **1998**, *99*, 391.
(86) te Velde, G.; Bickelhaupt, F. M.; Baerends, E. J.; Guerra, C. F.; van Gisbergen, S. J. A.; Snijders, J. G.; Ziegler, T. *J. Comput. Chem.* **2001**, *22*, 931.

quality (TZP). Electrons in orbitals up to and including 1s {C}, 2p {P, Cl} and 4d {Ru} were treated in accordance with the frozen-core approximation. Geometry optimizations employed the gradient algorithm of Versluis and Ziegler.[87] Functionals used in the optimization calculations were the local density approximation (LDA) to the exchange potential,[88] the correlation potential of Vosko, Wilk, and Nusair (VWN),[89] and the nonlocal corrections of Perdew, Burke, and Enzerhof (PBE).[90] Time-dependent calculations (TD-DFT) were also pursued on the PBE/TZP-optimized structures, using either PBE or the asymptotically correct functional of van Leeuwen and Baerends (LB94).

Z-Scan. Measurements were performed using an amplified femtosecond laser system consisting of a Clark-MXR CPA-2001 regenerative amplifier and a Light Conversion TOPAS optical parametric amplifier. The system was tuned in the range 520 to 1500 nm using the (pump + idler) sum frequency generation, second harmonic of the signal, second harmonic of the idler, or the signal from the parametric amplifier. The repetition rate of the regenerative amplifier was usually reduced to 98 Hz to minimize thermal effects[91] and sample decomposition. The pulse duration was typically about 150 fs. The required wavelength was separated from other components of the TOPAS output using polarizing optics and color glass filters, and the beam was suitably attenuated with neutral density filters to $\sim\mu$J/pulse range.

The Z-scan measurements were carried out in a standard setup adjusting the focusing to provide focal spots with a radius of $1/e^2$ intensity, w_0, being typically within the range 40−80 μm. This resulted in Rayleigh lengths greater than 3 mm, allowing measurements of solutions in 1 mm path glass cells (of the total thickness of ~3 mm including the glass walls) to be treated using the thin sample approximation. All measurements were calibrated against Z-scan measurements of the pure solvent as well as a 3 mm thick silica plate.[91] It has been assumed that dispersion of the nonlinear refractive index of silica can be neglected in the wavelength range employed, so it was assumed that $n_2 = 3 \times 10^{-16}$ cm^2 W^{-1} independent of the wavelength. The light intensity could then be determined from the measurement on the silica plate, and it was adjusted to about 50−100 GW cm^{-1} so that the nonlinear phase shift was in the range about 0.5−1.0 rad for most samples.

The compounds were dissolved in dichloromethane under a nitrogen atmosphere at concentrations in the range 0.1−1% w/w, and the solutions were placed in Starna glass cells with 1 mm path length, stoppered and sealed with Teflon tape. Tests with THF solutions showed a decreased photochemical stability compared to the CH_2Cl_2 solutions. Because of experimental limitations, a single concentration of each compound was examined. For each experiment, the real and imaginary part of the nonlinear phase shift was determined by numerical fitting using a computational procedure based on equations derived by Sheikh-bahae et al.,[92] and the real and imaginary part of the solute hyperpolarizability was calculated by assuming additivity of the nonlinear properties of the solutions.

Results and Discussion

Syntheses of Alkynes. Several new arylalkynes were prepared as precursors for the metal-containing OPEs, the syntheses being summarized in Schemes 1−3. Moore and co-workers have demonstrated the utility of the triazene group to rapidly introduce an iodo substituent[93] and thereby minimize the need for trans-halogenation reactions. Following this approach, the 1-aryl-3,3-dipropyltriazenes **1** and **2** were prepared (Scheme 1). Sonogashira coupling of the bromo compound **1** and trimethylsilylacetylene gave the trimethylsilylethynyl derivative **3**, which was desilylated to afford the ethynyl derivative **4**. Subsequent coupling of **4** to 1-iodo-4-(trimethylsilylethynyl)benzene afforded **5**, which was heated at 110 °C in iodomethane to demask the compound, affording the iodo derivative **6**. Similarly, **2** and 1-ethynyl-4-(triisopropylsilylethynyl)benzene were coupled under Sonogashira conditions to give **7**, subsequent heating in iodomethane affording **8**. Other new di-, tri-, penta-, hepta-, and nona(phenyleneethynylenes) were prepared by similar combinations of Sonogashira coupling, desilylation, and trans-halogenation reactions (Schemes 2 and 3), the incorporation of one to three 2,5-di(hexyloxy) phenyl rings ensuring solubility of both the organic compounds and their organometallic derivatives.

Scheme 1[a]

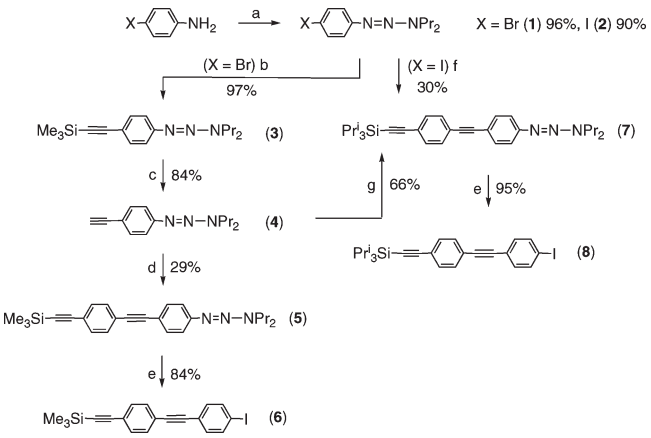

[a] (a) (i) HCl (2.3 equiv), $NaNO_2$ (1.5 equiv), 30 min, 0°C. (ii) $NHPr^n_2$, K_2CO_3. (b) $Me_3SiC{\equiv}CH$ (1.5 equiv), $PdCl_2(PPh_3)_2$ (4%), CuI (2%), NEt_3, reflux overnight. (c) $(NBu^n_4)F$ (1.1 equiv), CH_2Cl_2, 15 min. (d) 4-$Me_3SiC{\equiv}CC_6H_4I$, $PdCl_2(PPh_3)_2$ (4%), CuI (2%), NEt_3, RT, 4 h. (e) MeI, 110°C, 10 h. (f) 4-$Pr^i_3SiC{\equiv}CC_6H_4C{\equiv}CH$, $Pd(PPh_3)_4$ (4%), CuI (2%), NEt_3, RT, 4 h. (g) 4-$Pr^i_3SiC{\equiv}CC_6H_4Br$, $PdCl_2(PPh_3)_2$ (4%), CuI (3%), NEt_3, reflux overnight.

Syntheses of Metal Alkynyl Complexes. The syntheses of the new metal-containing OPEs are summarized in Schemes 4−7. Metal complexation of the OPEs with *cis*-$RuCl_2L_2$, extending a procedure originally developed by Dixneuf and co-workers,[94−97] afforded the alkynyl complexes **18**−**24** in satisfactory yield (Scheme 4). The terminal alkynes **10**, **12**, and **16** are less stable than the internal alkynes prepared in this study, which has frustrated attempts to obtain satisfactory microanalyses, but they are

(87) Versluis, L.; Ziegler, T. *J. Chem. Phys.* **1988**, *88*, 322.
(88) Parr, R. G.; Yang, W. *Density Functional Theory of Atoms and Molecules*; Oxford University Press: New York, 1989.
(89) Vosko, S. H.; Wilk, L.; Nusair, M. *Can. J. Phys.* **1980**, *58*, 1200.
(90) Perdew, J. P.; Burke, K.; Ernzerhof, M. *Phys. Rev. Lett.* **1996**, *77*, 3865.
(91) Samoc, M.; Samoc, A.; Luther-Davies, B.; Humphrey, M. G.; Wong, M.-S. *Opt. Mater.* **2003**, *21*, 485.
(92) Sheik-Bahae, M.; Said, A. A.; Wei, T.; Hagan, D. J.; van Stryland, E. W. *IEEE J. Quantum Electron.* **1990**, *26*, 760.
(93) Moore, J. S.; Weinstein, E. J.; Wu, Z. *Tetrahedron Lett.* **1991**, *32*, 2465.
(94) Touchard, D.; Morice, C.; Cadierno, V.; Haquette, P.; Toupet, L.; Dixneuf, P. H. *J. Chem. Soc., Chem. Commun.* **1994**, 859.
(95) Guesmi, S.; Touchard, D.; Dixneuf, P. H. *Chem. Commun.* **1996**, 2773.
(96) Touchard, D.; Haquette, P.; Daridor, A.; Romero, A.; Dixneuf, P. H. *Organometallics* **1998**, *17*, 3844.
(97) Touchard, D.; Guesmi, S.; Pichon, L. L.; Daridor, A.; Dixneuf, P. H. *Inorg. Chim. Acta* **1998**, *280*, 118.

Scheme 2[a]

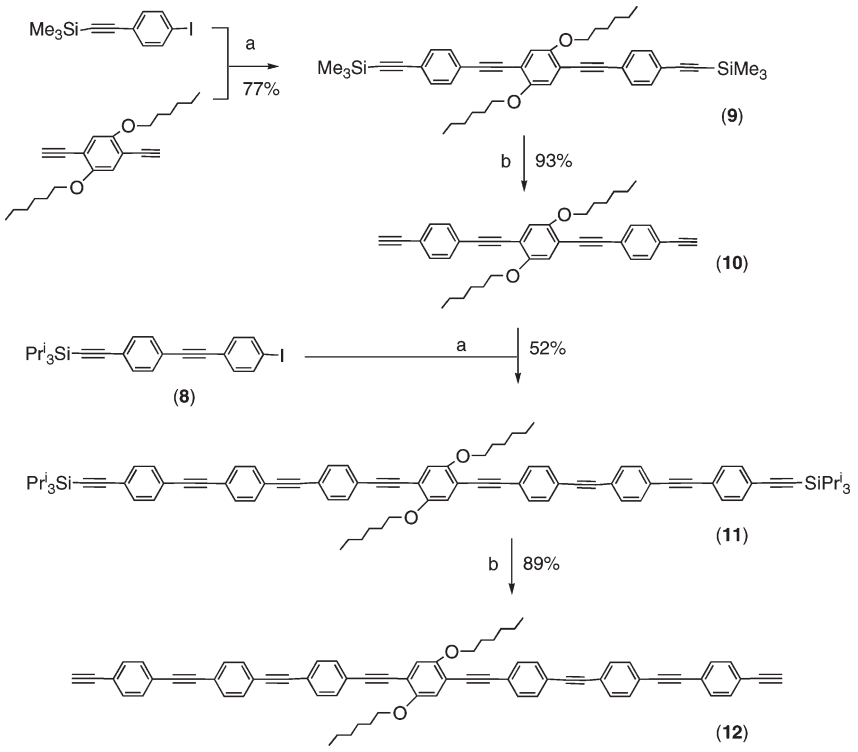

[a] (a) $PdCl_2(PPh_3)_2$ (1%), CuI (1%), NEt_3, RT, 48 h. (b) $(NBu^n_4)F$, CH_2Cl_2, 15 min.

Scheme 3[a]

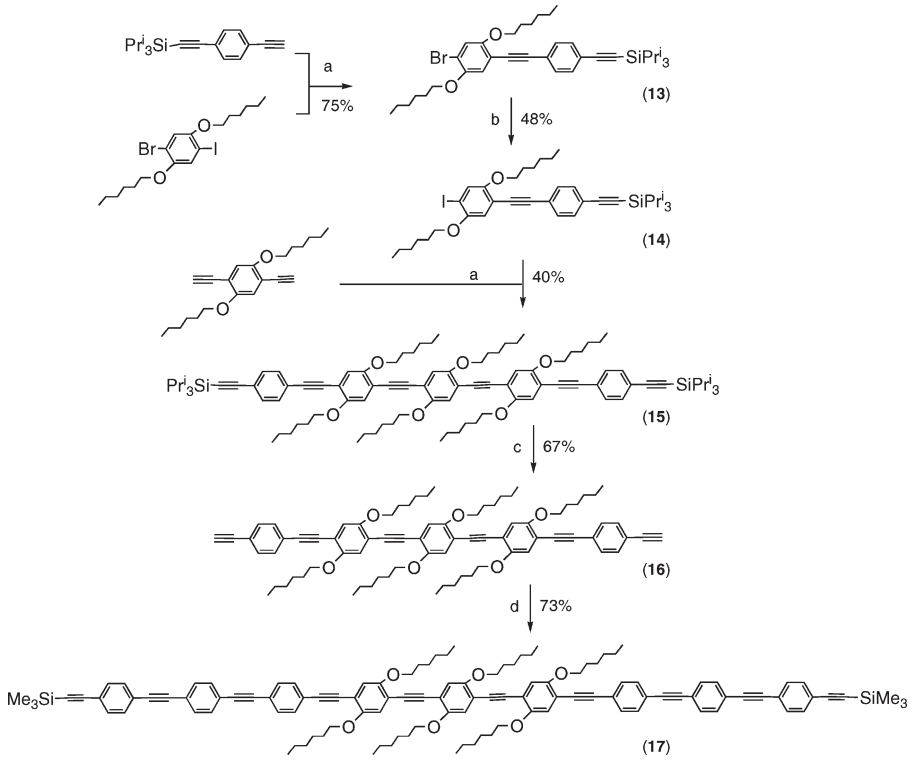

[a] (a) $PdCl_2(PPh_3)_2$ (2-3%), CuI (1-7%), NEt_3, RT, 48 h. (b) Bu^nLi, I_2, THF. (c) $(NBu^n_4)F$, CH_2Cl_2, RT, 15 min. (d) 4-$Me_3SiC{\equiv}CC_6H_4C{\equiv}C$-4-$C_6H_4I$ (**6**), $PdCl_2(PPh_3)_2$ (1%), CuI (2%), NEt_3, RT, 48 h.

of sufficient stability to permit us to prepare **19**, **20**, **23**, and **24** in fair to good yield. The product from the desilylation of **17** was less stable than other terminal alkynes prepared in the current studies, but the metal-terminated nona(phenyleneethynylene) **25** could still be prepared in low, but acceptable, yield, by in situ desilylation and

Scheme 4[a]

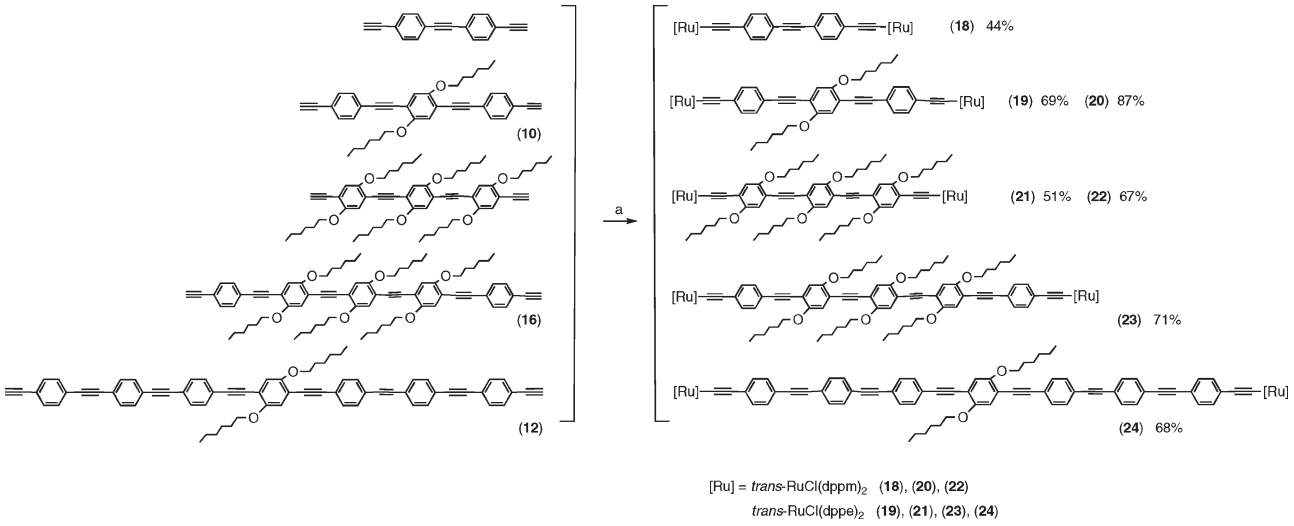

[a] (a) (i) *cis*-$RuCl_2(dppm)_2$ or *cis*-$RuCl_2(dppe)_2$, $NaPF_6$, or NH_4PF_6, CH_2Cl_2, reflux 16 h. (ii) NEt_3.

Scheme 5

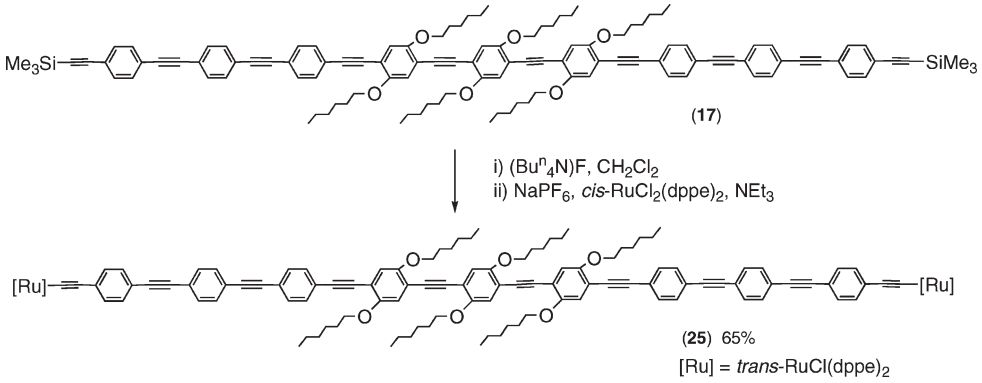

Scheme 6[a]

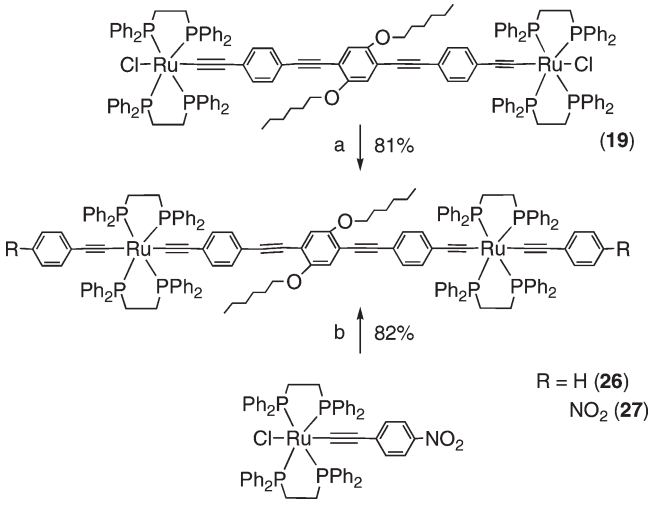

[a] (a) Phenylacetylene, $NaPF_6$, NEt_3, reflux 1 h. (b) 2,5-(HC≡CC_6H_4-4-C≡C)$_2$-1,4-{$Me(CH_2)_5O$}$_2C_6H_2$ (**10**), $NaPF_6$, NEt_3, reflux 16 h.

immediate complexation (Scheme 5). The penta(phenyleneethynylene)s **26** and **27**, in which the ligated metal centers are attached to a central trimer unit but have differing phenylethynyl termini, were prepared from different precursors. While **19** was reacted successfully with phenylacetylene to give **26**, attempts to couple **19** with 4-nitrophenylacetylene were unsuccessful; the target complex **27** was subsequently synthesized from reaction of two equivalents of *trans*-[Ru(C≡CC_6H_4-4-NO_2)Cl(dppe)$_2$] with **10** (Scheme 6). Further examples of OPEs with ligated metal units in the OPE chain rather than at the periphery were prepared by the same approach, that is, reaction of the metal-terminated OPEs **19** and **23** with 4-(phenylethynyl)phenylacetylene to afford **28** and **29**, respectively (Scheme 7).

The new compounds were characterized by MS and NMR, IR, and UV−vis spectroscopies, the last-mentioned being discussed in detail below. The ^{31}P NMR spectra contain singlets, confirming the *trans*-disposed alkynyl and chloro/alkynyl ligands, with chemical shifts that are sensitive to the environment around the ruthenium center. Complexes containing a $Ru(dppm)_2$ unit with one chloro and one alkynyl ligand attached in a *trans* arrangement (**18**, **20**, and **22**) show a singlet in the range −5 to −6 ppm, whereas phosphorus nuclei of the dppe analogues (**19**, **21**, **23**, **24**, and **25**) resonate in the range 49 to 50 ppm. In contrast, the ^{31}P NMR spectra of the ruthenium bis-alkynyl complexes (**26**, **27**, **28**, and **29**) contain a phosphorus resonance at about 54 ppm. The IR ν(C≡C)Ru bands for the monoalkynyl complexes (**18**, **19**, **21**−**25**) appear in the

Scheme 7

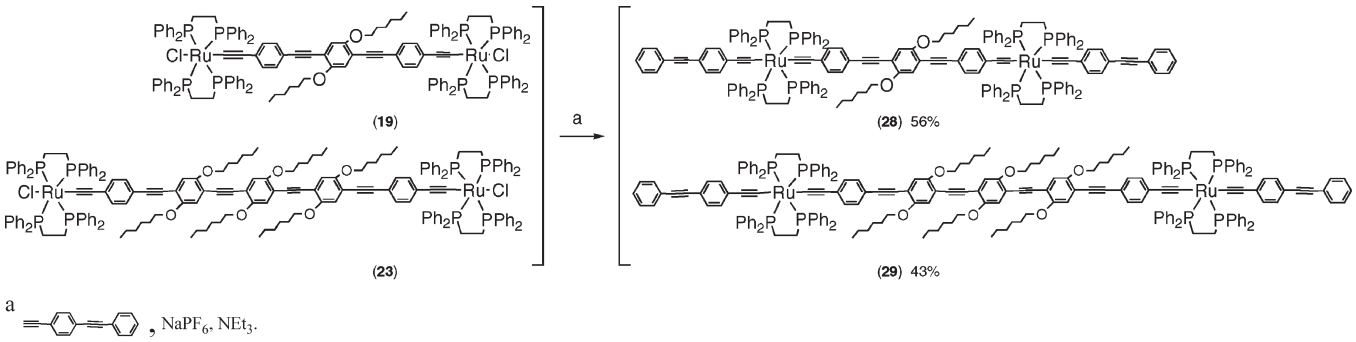

range 2059 to 2068 cm^{-1}; for the bis-alkynyl complexes (**26**, **27**, **29**), this band is shifted to lower frequencies, being found in the range 2046 to 2057 cm^{-1}.

Linear Optical Properties. The major interest of the present study is the effect on optical properties (linear and nonlinear) of ligated metal incorporation at specific sites in an OPE. There are several molecular modifications inherent in this set of complexes, the impact of which we have sought to deconvolute. Figure 1 illustrates the effect of incorporation of solubilizing substituents. Replacing phenylene units in the OPE bridge by 2,5-di(hexyloxy)-phenylene groups in proceeding from 1,4-{*trans*-[RuCl-(dppe)$_2$]C≡CC_6H_4-4-C≡C}$_2C_6H_4$ (**30**) to **19** and then **21** (Figure 1) results in a red shift of the low-energy maximum at about 22000 cm^{-1}; at higher energy (ca. 32000 cm^{-1}), the spectra suggest bands corresponding to alkoxy-containing rings at about 33000 cm^{-1} (**19** and **21**) and phenylene rings at about 31000 cm^{-1} (**19** and **30**). The effect of coligand variation is explored in Figure 2, replacement of dppm by dppe in proceeding from **22** to **21** resulting in little change in the optical spectra. Peripheral group modification is examined in Figure 3, replacement of chloro by phenylethynyl and then phenylethynyl-4-phenylethynyl ligand, in progressing from **19** to **26** and then **28**, blue-shifting the low-energy maximum; incorporation of a 4-nitro substituent (in proceeding from **26** to **27**) introduces a new low-energy component at 20000 cm^{-1}.

The effect of extending the OPE chain is examined in Figure 4. Incorporating additional phenyleneethynylene units results in a blue shift of the low-energy band. Varying the location of the ligated metal center in a fixed length OPE results in little change in the low-energy band as the metal moves to the periphery (Figure 5); note that the pairs of complexes are not isomers, but rather differ in peripheral Cl versus H atom.

Computational Studies. These trends in optical properties were probed theoretically. In the discussion that follows, we consider a single-photon transition to be significantly allowed if it has a calculated oscillator strength *f* of 0.1 or greater. [It should be noted that the computed oscillator strengths are expected to be indicative rather than prescriptive, and that the two TD-DFT methods employed here routinely deliver oscillator strengths for individual transitions that differ by a factor of 2 or more: nonetheless, the set of significantly allowed transitions for any species is generally similar for both methods. For the systems under investigation here, LB94-computed excitation energies are typically 5−10% lower than those determined using PBE, and it is likely that both methods significantly underestimate the true excitation energies (perhaps by as much as 20%). Nevertheless, it is expected that the results obtained using either LB94 or PBE are internally consistent, so that the trends observed in comparing the spectra computed for different species should be pertinent to interpretation of the experimentally determined spectra of these species and their laboratory analogues.]

For the series 0M*j*M0 (j = 3, 5, 7, 9) the lowest-energy transition decreases monotonically with increasing *j*, a result that holds for both the PBE and the LB94 TD-DFT methods. For 0M3M0, the lowest-energy significantly allowed transition is also the most intense (highest oscillator strength *f*) transition across the range from 0 to 35000 cm^{-1}, but for the larger 0M*j*M0 species there are generally several transitions below about 30000 cm^{-1} that possess larger *f* values than the lowest-energy transition. The molecular orbitals principally implicated in the lowest-energy transition are the acetylenic-character highest occupied molecular orbital (HOMO), dominantly distributed across the C_2 units immediately inward from the Ru atoms, and the cumulenic lowest unoccupied molecular orbital (LUMO), which is mainly localized among the phenylethynyl linkages nearest to the molecule's center-of-symmetry.

While the lowest-energy transition does not remain the highest *f*-value transition as the central oligo(phenyleneethynylene) length *j* is increased, there is an identifiable unifying feature of the maximal *f*-value transitions, which are either "*n*HOMO"→LUMO (where "*n*HOMO", the next highest-lying occupied orbital *of the same symmetry* as the HOMO, is acetylenic in character and localized near the molecule's center-of-symmetry) or HOMO→"*n*LUMO" (where "*n*LUMO", the next lowest-lying virtual orbital *of the same symmetry* as the LUMO, is cumulenic and displaced further away from the molecule's center). Thus in all instances the highest *f* transitions involve excitation from acetylenic to cumulenic molecular orbitals that are not greatly spatially separated from each other. Figure 6 displays the crucial orbitals for the typical case of 0M7M0.

Calculations on several di- and hexamethoxylated species were also undertaken. In all instances, these models were constructed in such a way as to preserve C_{2v} symmetry within the structure, with $(OMe)_2$ derivatives involving functionalization of the central phenylene ring

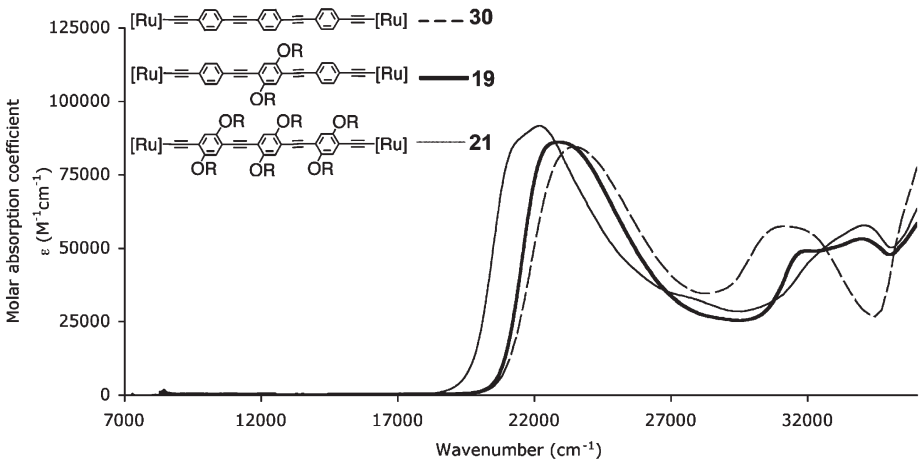

Figure 1. UV−vis−NIR spectra of **30**, **19**, and **21** in CH_2Cl_2, illustrating the effect of introduction of solubilizing substituents. [Ru] ≡ *trans*-[RuCl(dppe)$_2$].

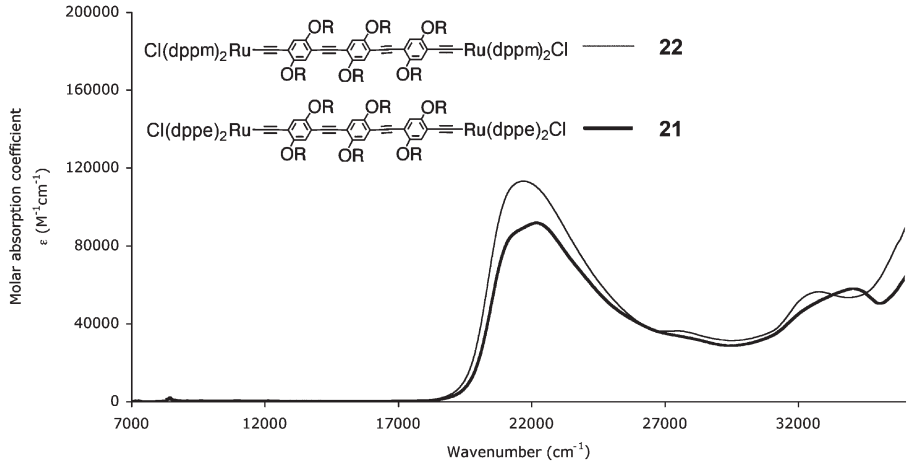

Figure 2. UV−vis−NIR spectra of **22** and **21** in CH_2Cl_2, illustrating the effect of coligand modification.

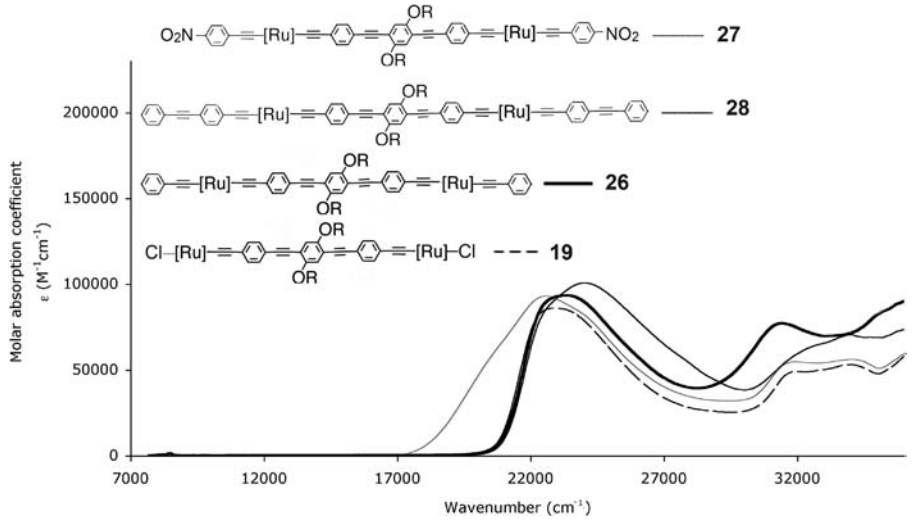

Figure 3. UV−vis−NIR spectra of **27**, **28**, **26**, and **19** in CH_2Cl_2, illustrating the effect of peripheral group modification. [Ru] ≡ *trans*-[Ru(dppe)$_2$].

and $(OMe)_6$ derivatives featuring dimethoxylation of each of the three phenylene rings closest to the molecule's center of symmetry. Methoxy substituents were employed as a smaller analogue of the hexyloxy derivatives prepared in the laboratory. Comparison of the calculated spectral features of dimethoxylated and dihexyloxylated 0M3M0 revealed a very close match across the spectrum, indicating to us that OMe is an effective model for the larger hexyloxy substituent. The methoxylation of the various model complexes yields spectra that do not differ greatly from those of their "unadorned" 0M*j*M0 analogues, but which at first glance show small

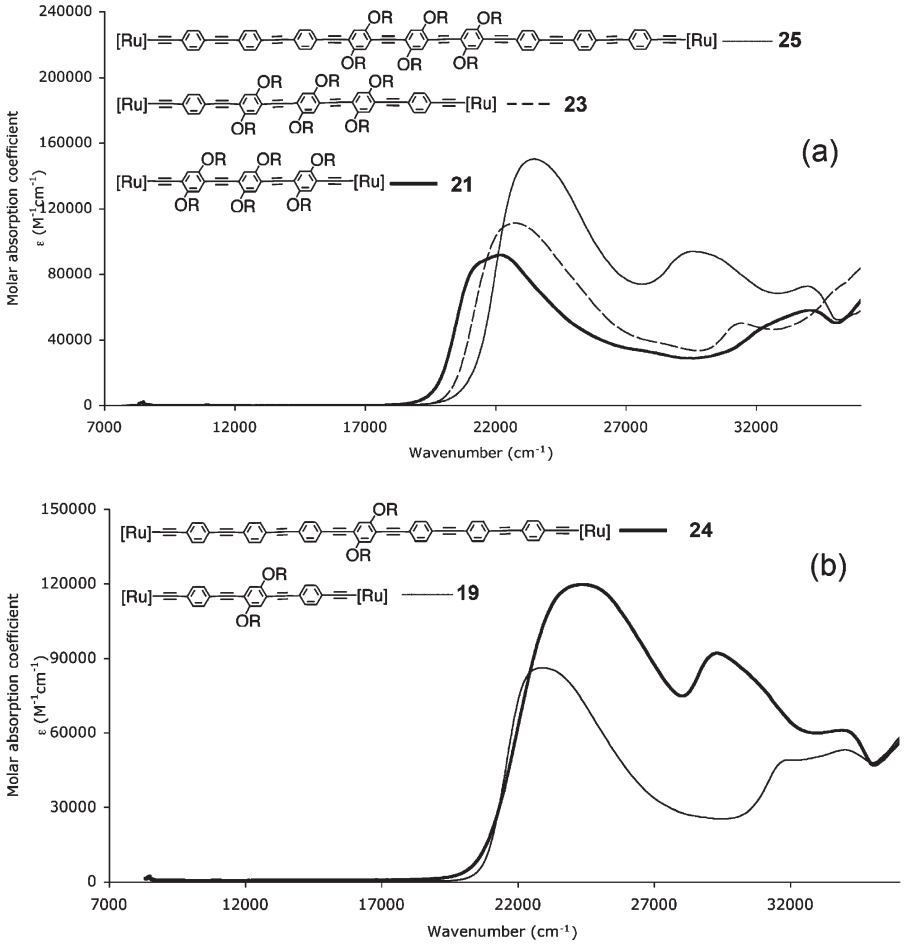

Figure 4. UV−vis−NIR spectra of **24** and **19** in CH_2Cl_2, illustrating the effect of chain lengthening. [Ru] ≡ *trans*-[RuCl(dppe)$_2$].

and inconsistent shifts in transition frequencies, with some strong transitions red-shifted and others blue-shifted by a small to moderate extent. Closer inspection of the shifted transitions, particularly for the larger complexes ($j \geq 5$), reveals that methoxylation produces a blue-shift when the transition involves excitation from a peripheral OMO to a more central UMO, but a red-shift when the UMO is further displaced from the molecule's center of symmetry. Thus alkoxylation, introduced into the laboratory structures as an aid to solubility, has a modest but distinct influence on orbital energies and on the observed spectra.

The model set also allows us to explore the spectral consequence of shifting the Ru-containing moieties along the complex's backbone. The most extended sequence of such data is obtained for the *i*M*j*M*i* species, where $2i + j = 9$: 0M9M0, 1M7M1, 2M5M2, 3M3M3, and 4M1M4. The frontier orbitals for these species suggest that the OPE backbones are electronically partitioned into "domains" between which the axial Ru atoms act as natural dividers across which little or no frontier-electronic leakage occurs. In 0M9M0, there are no peripheral "domains" but the central domain is sufficiently large that, as noted above, the most intense transitions are not apparently HOMO → LUMO but instead involve frontier orbitals of closer spatial distribution. This trend is also adhered to as the peripheral domains are built up at the expense of the central domain, but across 0M9M0, 1M7M1, 2M5M2, and 3M3M3 the lowest-energy, as well as the most intense transition, remain effectively focused on the progressively diminishing central domain. It is only for 4M1M4 (where the short central domain nevertheless retains both the HOMO and the LUMO) for which the most intense transition is located along the extended peripheral domains.

The tendency for increasing OPE chain length to result in a red-shifting of the most intense transition is significantly at odds with the experimental results reported here. While the underlying causes of this discrepancy are not certain, one likely contributing factor is that our calculations have predominantly been conducted on configurations of D_{2d} (*i*M*j*M*i*) or C_{2v} (methoxylated *i*M*j*M*i*) symmetry, for reasons of computational expediency. These symmetry constraints ignore the opportunities for rotation of phenylene moieties around the central rotational axes of the structures. Thus, while our primary calculations concern structures with a highly coplanar arrangement of the phenylene moieties, this may not reflect the statistically averaged structures under laboratory conditions. To test this possibility, we have also performed calculations on the influence of two sample rotational modes (corresponding to rotation of the central $C_6H_4-C\equiv C-C_6H_4-C\equiv C-C_6H_4$ fragment within 2M5M2, and to rotation of the peripheral $C_6H_5-C\equiv C-C_6H_4-C\equiv C-C_6H_4$ fragments within 4M1M4) at deviations from coplanarity ranging from 5° to 90°. Two important results emerge from these

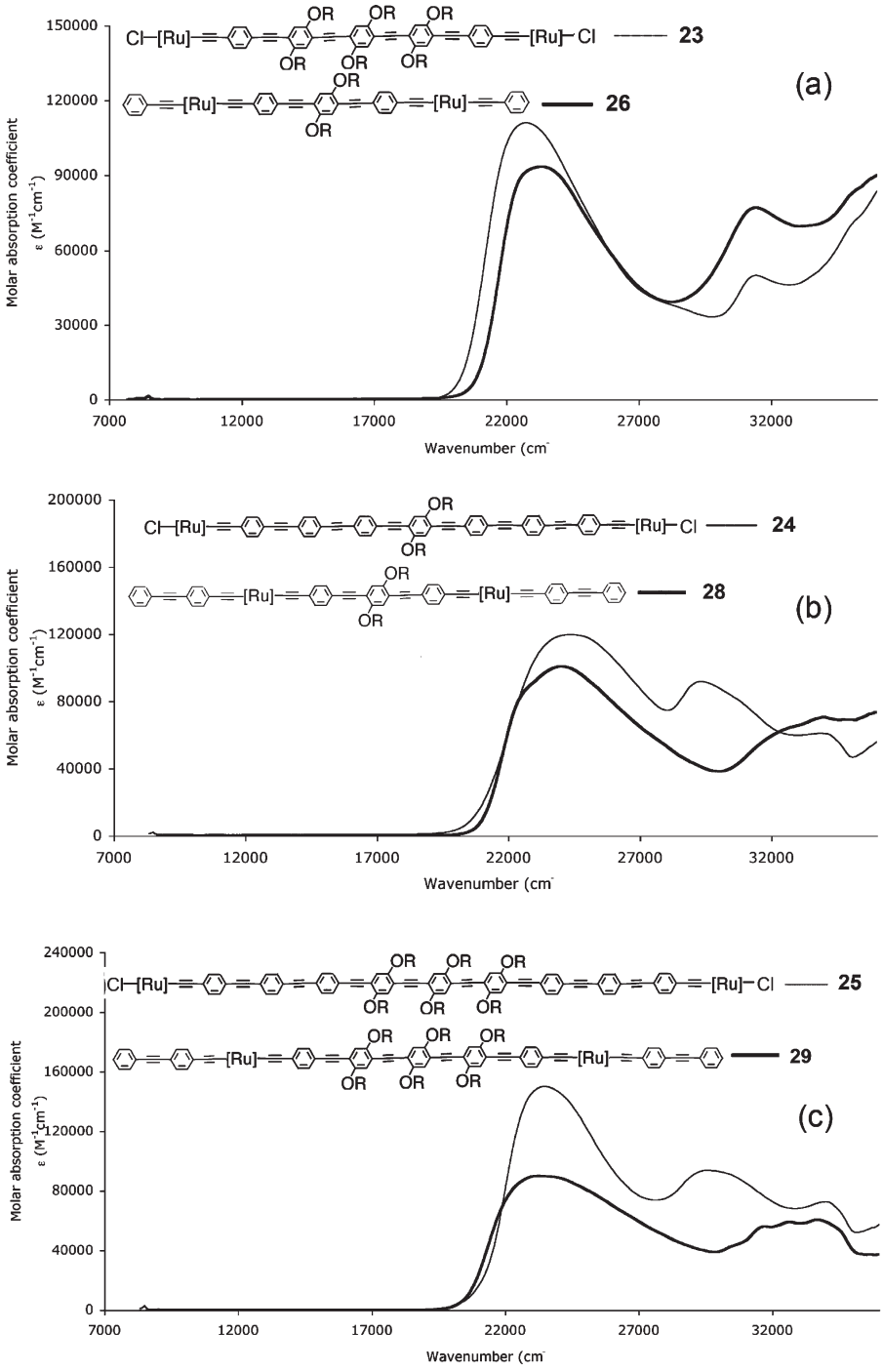

Figure 5. UV−vis−NIR spectra of (a) **23** and **26**, (b) **24** and **28**, and (c) **25** and **29** in CH_2Cl_2, illustrating the effect of metal location modification. [Ru] ≡ *trans*-Ru(dppe)$_2$].

calculations. First, the barrier to rotation appears to be generally low, of the order 7−10 kJ mol^{-1} for traversal of the (90°) transition state and thus it is reasonable to expect that significant distortions from fully coplanar structures will be common, particularly for the larger oligomers, among the range of conformers comprising the laboratory samples. Second, while the impact of rotation on the frequency of individual transitions is generally very small (a 30° tilt from coplanarity changes the frequency of most transitions by less than 200 cm^{-1}), and is more often evidenced as a mild *red-shifting* of the individual spectral features (consistent with a greater rotation-induced destabilization of generally bonding occupied molecular orbitals than on generally non- or antibonding virtual orbitals), the influence of rotation on relative intensities of neighboring transitions can be significantly more dramatic, with a 30° tilt often sufficient to cause a greater-than-2-fold shift in the relative intensities of prominent adjacent transitions. Since this phenomenon often favors the higher-energy transition within a closely spaced pair, and since the opportunities for internal rotation are increased by increasing chain length, we propose that the laboratory observation of blue-shifting may arise because the observed spectral envelope generally consists of several

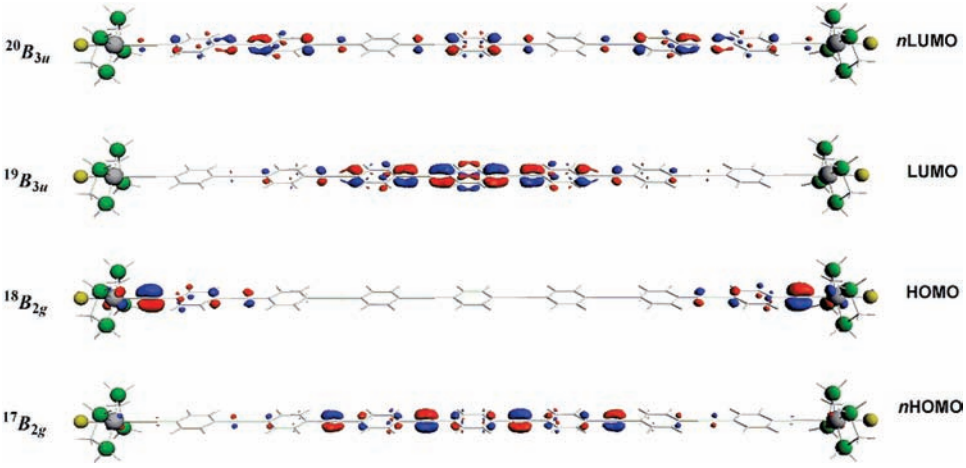

Figure 6. Depiction of orbitals contributing to the most intensely allowed (highest calculated *f*-value) single-photon transitions for 0M7M0. The features of these orbitals—acetylenic-character HOMO and the lower-lying $^{17}B_{2g}$ orbital of the same symmetry ("*n*HOMO"), and cumulenic LUMO and the symmetry-related $^{20}B_{3u}$ orbital ("*n*LUMO"), with the lower-lying orbital of each type having its electron density concentrated toward the molecule's center-of-symmetry—are broadly consistent with trends evident across the range of *i*M*j*M*i* structures explored here.

overlapping transitions, whose individual reactions to thermally driven internal rotations are markedly different.

Nonlinear Optical Properties. The cubic NLO properties of a selection of the preceding compounds were assayed over a wide range of visible and infrared wavelengths. As can be seen in Figure 7a and Supporting Information, Figures S1a−S5a, the studies were carried out with the incident wavenumber in an essentially transparent region of the one-photon (UV−vis−NIR) spectrum, which is 8000−19000 cm^{-1} for all of the compounds studied. The short wavelength limit of the measurements coincided with the onset of strong one-photon absorption (1PA), because strong 1PA precludes measurement of NLO properties by a transmission technique (it should be noted that samples for Z-scan measurements need to be relatively highly concentrated compared to solutions used for one-photon spectra). Some data were obtained in regions of moderate 1PA by applying appropriate correction factors,[92] but the results carry inherently large experimental errors.

The Z-scan experiment allows simultaneous evaluation of the real (nonlinear refraction) and imaginary (nonlinear absorption) part of the cubic hyperpolarizability, but the accuracy of the determination of the real part is much lower than that of the imaginary part. This is a result of the refractive nonlinearity of the solute being measured as an increment to the refractive nonlinearity of the solvent and cuvette while the nonlinear absorption of the solvent is negligible in the wavenumber and intensity ranges used, so the absorptive component of the nonlinearity of the solute is determined in a background-free manner. The measurement inaccuracies become a much greater problem at lower concentrations of complex as in the case of complexes **24** and **28**, which were not soluble enough for accurate Z-scan measurements. This highlights the necessity of the di(hexyloxy)-substituents even though they affect the absorption.

In principle, interpretation of the dispersion of nonlinearities requires knowledge of both the structure of the energy levels of the complexes and the strengths of a multitude of transitions between them. A complication is that the expressions describing the cubic nonlinear optical effects treated within a perturbation approach[98,99] contain terms that may be both positive and negative (thus compensating for each other). In contrast to the case of 1PA spectra (and the related dispersion of the linear polarizability of the molecules), the terms in the cubic NLO expressions contain integrals that do not disappear for transitions between states of the same symmetry. This means that, for centrosymmetric molecules, the two-photon absorption (2PA) spectra may be substantially different from the one-photon absorption spectra because final states of different parity will be involved. Nevertheless, as a first attempt to understand the dispersion of γ and σ_2, the complex hyperpolarizability frequency dependence can be compared to the one-photon spectrum at twice the wavenumber of the two-photon incident light, since, for large molecules with a large number of close-lying excited states, a 2PA peak close to half the wavenumber of the lowest 1PA transition may be intuitively expected even though the symmetry rules for the transitions are different.[100] Figure 7a,b illustrates this for **21**. It can be seen that there is no appreciable two-photon absorption (imaginary part of γ) until twice the wavenumber of the incident light reaches the wavenumber corresponding to the onset of the first absorption band. On the other hand, the frequency dependence of the imaginary part of γ does differ from that of the 1PA coefficient, indicating that there may be some strongly allowed two-photon active states at higher energies (the peak of the two-photon absorption is at a final state energy of about 23000 cm^{-1}, which corresponds to incident photons of 11500 cm^{-1}). The real part of γ shows a dispersion behavior that appears to be in a Kramers−Kronig-like relationship to that of the imaginary part. As discussed by some of the present authors,[101,102] such behavior may be expected when the

(98) Orr, B. J.; Ward, J. F. *Mol. Phys.* **1971**, *20*, 513.
(99) Dirk, C. W.; Cheng, L. T.; Kuzyk, M. G. *Int. J. Quantum Chem.* **1992**, *43*, 27.
(100) Powell, C. E.; Morrall, J. P. L.; Ward, S. A.; Cifuentes, M. P.; Notaras, E. G. A.; Samoc, M.; Humphrey, M. G. *J. Am. Chem. Soc.* **2004**, *126*, 12234.
(101) Samoc, M.; Samoc, A.; Humphrey, M. G.; Cifuentes, M. P.; Luther-Davies, B.; Fleitz, P. A. *Mol. Cryst. Liq. Cryst.* **2008**, *485*, 146.
(102) Samoc, M.; Samoc, A.; Dalton, G. T.; Cifuentes, M. P.; Humphrey, M. G.; Fleitz, P. A. *Proc. SPIE, Int. Soc. Opt. Eng.* **2008**, *6801*, 68011O-1–6.

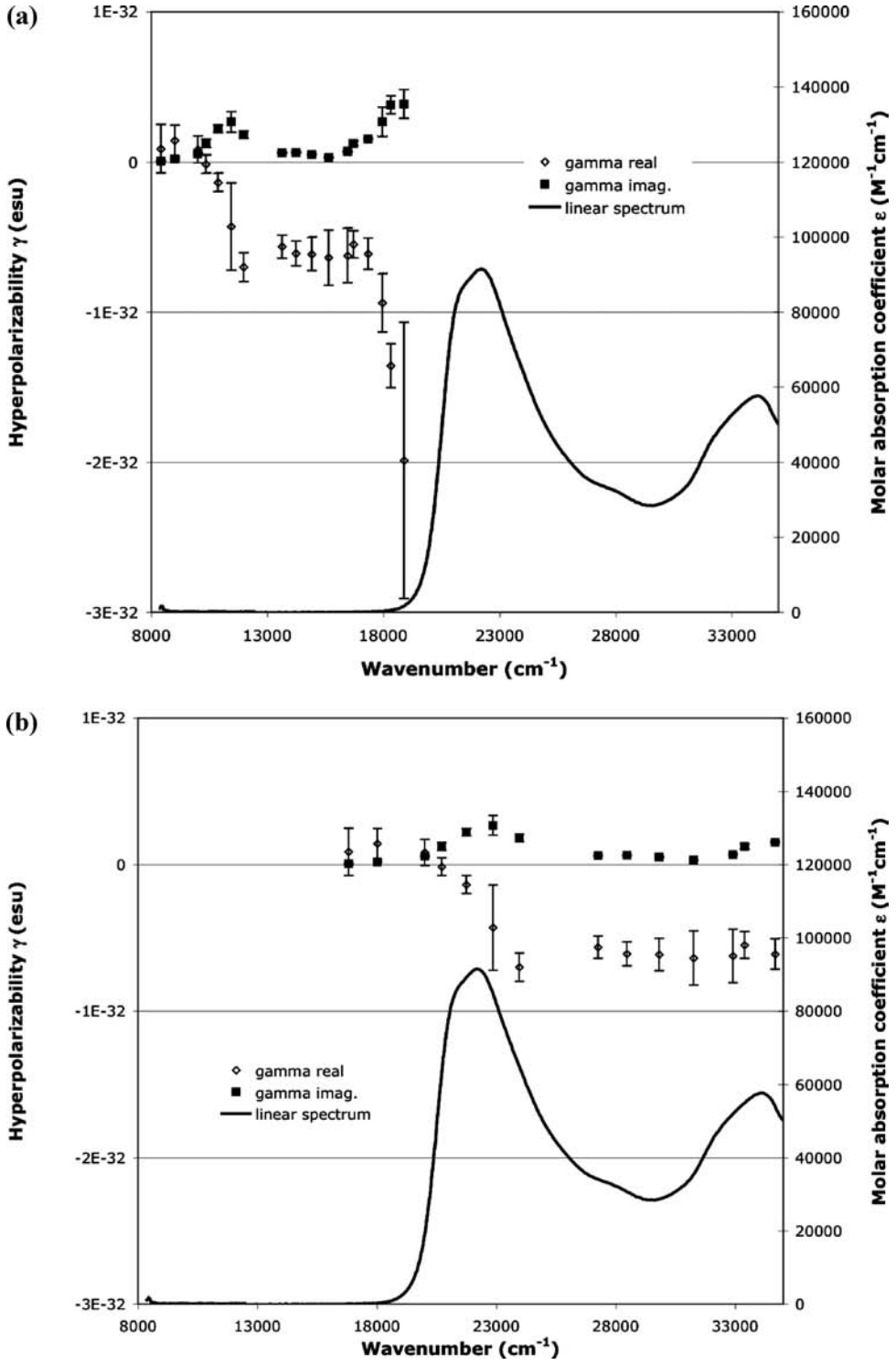

Figure 7. Comparison of the linear optical spectra to the nonlinear optical spectra for 2,5-[5-{*trans*-[RuCl(dppe)$_2$]C≡C}-1,4-{Me(CH$_2$)$_5$O}$_2$C$_6$H$_2$-2-C≡C]$_2$-1,4-{Me(CH$_2$)$_5$O}$_2$C$_6$H$_2$ (**21**) in CH_2Cl_2 solvent. (a) Nonlinear optical spectra plotted at the incident wavenumber. (b) Nonlinear optical spectra plotted at twice the incident wavenumber.

hyperpolarizability is dominated by a single 2PA transition, but more complicated cases abound, as can be seen by inspection of the dispersion curves in Figure 7 and Supporting Information, Figures S1−S5. An increase of the imaginary part of γ, coincidental with an increase in the one-photon spectrum, is also seen in **21** at 32000 cm^{-1}, **23** at 31000 cm^{-1}, **26** at 31000 cm^{-1}, **28** at 32000 cm^{-1}, and **29** at 32000 cm^{-1}.

Table 1 lists the maximum values of the real and imaginary parts of γ, as well as the two-photon cross sections of the compounds. It is immediately apparent that the nonlinear absorption behavior is in stark contrast to the trends in linear absorption. While the 1PA maximum undergoes a blue shift upon OPE bridge lengthening (Figure 4), the 2PA peak remains invariant on proceeding from **21** to **23** and then **25** or from **28** to **29**.

Table 1. Linear Optical and Nonlinear Optical Parameters of Selected Metal-Containing OPEs

compound	1PA peak maximum (cm^{-1}) [ε, 10^4 M^{-1} cm^{-1}][a]	2PA peak maximum (cm^{-1})[a]	γ_{imag} (10^{-36} esu)[a]	σ_2 (GM)[a]	γ_{real} peak maximum (cm^{-1})[a]	γ_{real} (10^{-36} esu)[a]
1,4-{*trans*-[RuCl(dppm)$_2$]C≡C}$_2$C$_6$H$_4$ (**31**)	28400 [2.87]	15800	2100	600	14500	1000
					17360	−630
2,5-[5-{*trans*-[RuCl(dppe)$_2$]C≡C}-1,4-{Me(CH$_2$)$_5$O}$_2$C$_6$H$_2$-2-C≡C]$_2$-1,4-{Me(CH$_2$)$_5$O}$_2$C$_6$H$_2$ (**21**)	22200 [9.14]	11430	2700	530	12000	−7000
2,5-[5-{*trans*-[RuCl(dppe)$_2$]C≡C-4-C$_6$H$_4$C≡C}-1,4-{Me(CH$_2$)$_5$O}$_2$C$_6$H$_2$-2-C≡C]$_2$-1,4-{Me(CH$_2$)$_5$O}$_2$C$_6$H$_2$ (**23**)	22800 [11.1]	11430	3000	580	12000	−9800
2,5-{*trans*-[RuCl(dppe)$_2$]C≡C(4-C$_6$H$_4$C≡C)$_3$}$_2$-1,4-{Me(CH$_2$)$_5$O}$_2$C$_6$H$_2$ (**24**)	24300 [12.0]	11430	3700	730	[b]	[b]
2,5-{5-(*trans*-[RuCl(dppe)$_2$]-C≡C(4-C$_6$H$_4$C≡C)$_3$}-1,4-{Me(CH$_2$)$_5$O}$_2$C$_6$H$_2$-2-C≡C}$_2$-1,4-{Me(CH$_2$)$_5$O}$_2$C$_6$H$_2$ (**25**)	23500 [15.0]	11430	3000	630	14900	−12000
2,5-{*trans*-[Ru(C≡CPh)(dppe)$_2$]C≡CC$_6$H$_4$-4-C≡C}$_2$-1,4-{Me(CH$_2$)$_5$O}$_2$C$_6$H$_2$ (**26**)	23400 [9.33]	11430	1430	300	10870	1200
					14900	−3400
2,5-{*trans*-[Ru(C≡CC$_6$H$_4$-4-C≡CPh)(dppe)$_2$]C≡CC$_6$H$_4$-4-C≡C}$_2$-1,4-{Me(CH$_2$)$_5$O}$_2$C$_6$H$_2$ (**28**)	24100 [10.1]	11430	1440	290	[b]	[b]
2,5-[5-(*trans*-[Ru(C≡CC$_6$H$_4$-4-C≡CPh)(dppe)$_2$]C≡C-4-C$_6$H$_4$C≡C)-1,4-{Me(CH$_2$)$_5$O}$_2$C$_6$H$_2$-2-C≡C]$_2$-1,4-{Me(CH$_2$)$_5$O}$_2$C$_6$H$_2$ (**29**)	23300 [8.97]	11430	5200	1050	12000	−9400

[a] CH_2Cl_2 solvent. [b] Values not available because of large error margins on data.

The 2PA peak is also invariant on peripheral OPE lengthening (proceeding from **26** to **28** or from **23** to **29**), although this structural modification shifts the 1PA peak (Figure 3). While the hexyloxy groups modify the linear optical spectra and location of $1PA_{max}$ (Figure 1), the presence or otherwise of these solubilizing substituents has no effect on the 2PA peak location, with the $2PA_{max}$ for **24** at the same frequency as that of **21**, **23**, and **25**. Metal location has little effect on the frequency of $1PA_{max}$ (Figure 5) and a similar lack of impact on the $2PA_{max}$ location (proceeding from **24** to **28** or from **25** to **29**). Indeed, the one structural modification that influences the frequency of the 2PA maximum is reduction of the OPE bridge length to a 1,4-diethynylbenzene unit, in proceeding to **31** [although **31** is a dppm-ligated complex, in contrast to the other complexes in the Z-scan study, we do not believe that this minor coligand modification will strongly influence optical properties, and this is reflected in the linear optical results (Figure 2)]. While the location of the 2PA maximum is largely invariant for these molecular modifications, the magnitude of the 2PA cross-section does vary. The errors associated with these data necessitate caution in interpretation, but the σ_2 value seems dependent on the metal-containing OPE size, the largest values being found for **29**, **24**, and **25**.

Discussion. The present studies have afforded a systematically varied series of OPEs incorporating metal centers in specific sites in the π-system. While mono- and di(phenyleneethynylene)s are quite soluble, solubility drops markedly at tri(phenylenenethynylene)s, which has necessitated the use of phenylene groups bearing solubilizing substituents to ensure that linear optical data and particularly nonlinear optical data for the complexes were accessible. The solubilizing substituents are essential to collect the spectral data, but they are not electronically innocent, so attempts to deconvolute their contribution were made.

The major interest in the present work is in understanding evolution in both 1PA and 2PA on varying the metal-containing OPEs. Delineating the factors influencing multiphoton absorption in organic systems has been a subject of considerable interest over the past few years.[103] While much attention has been directed at oligo(phenylenevinylene)s (OPVs) and OPEs for applications in molecular electronics and molecular photonics, OPEs possess the advantage of enhanced photostability. As a result, the 2PA properties of OPEs have come under scrutiny recently,[13,104−107] with a monotonic increase in σ_2 on OPE lengthening in some cases,[104,107] and no variation in others.[105] However, these studies report data at a single wavelength (800 nm) rather than the maximal values of σ_2, rendering development of structure−property relationships problematic.

The incorporation of metals into an OPE or OPV structure is of considerable interest in the nanoengineering of advanced functional materials. The intrinsic magnetic, electronic, and/or optical properties of ligated metal centers may be employed to tune or enhance the corresponding properties of the purely organic oligomer. The complexes in the present study comprise electron-rich metal centers linked by a π-delocalizable OPE bridge, and thus possess a D-π-D composition (D = donor) that has been identified as one of the more efficient structural motifs for optimizing 2PA cross-section. In contrast to the organic OPEs above, the incorporation of metal centers in the present work not only imparts important functionality (for example, optical nonlinearity can be reversibly switched under protic[108,109] or electrochemical control in ruthenium

(103) He, G. S.; Tan, L. S.; Zheng, Q.; Prasad, P. N. *Chem. Rev.* **2008**, *108*, 1245.
(104) Lo, P.; Li, K.; Wong, M.; Cheah, K. *J. Org. Chem.* **2007**, *72*, 6672.
(105) Yang, W. J.; Kim, C. H.; Jeong, M.-Y.; Lee, S. K.; Piao, M. J.; Jeon, S.-J.; Cho, B. R. *Chem. Mater.* **2004**, *16*, 2783.
(106) Weder, C.; Wrighton, M. S.; Spreiter, R.; Bosshard, C.; Günter, P. *J. Phys. Chem.* **1996**, *100*, 18931.
(107) Inokuma, Y.; Easwaramoorthi, S.; Jang, S. Y.; Kim, K. S.; Kim, D.; Osuka, A. *Angew. Chem., Int. Ed.* **2008**, *47*, 4840.
(108) Hurst, S.; Cifuentes, M. P.; Morrall, J. P. L.; Lucas, N. T.; Whittall, I. R.; Humphrey, M. G.; Asselberghs, I.; Persoons, A.; Samoc, M.; Luther-Davies, B.; Willis, A. C. *Organometallics* **2001**, *20*, 4664.
(109) Dalton, G. T.; Cifuentes, M. P.; Petrie, S.; Stranger, R.; Humphrey, M. G.; Samoc, M. *J. Am. Chem. Soc.* **2007**, *129*, 11882.

alkynyl complexes),[19,100,109−113] but in addition a bis (alkynyl)-ligated metal center can serve as an anchoring point for OPE segments, so developing an understanding of the influence of incorporation of the metal center is clearly important.

The linear optical properties in the metal-containing OPEs are strongly dependent on OPE length, solubilizing substituents at the bridging unit, and nature of the peripheral group appended to the metal centers. Unlike previous single-wavelength reports of systematically varied OPEs, the present wavelength-dependence studies, which are the first broad wavelength range studies of dispersion of the complex hyperpolarizability in such systems, have afforded the σ_2 maxima. In contrast to the 1PA dependencies, the location of the 2PA maximum is invariant for all metal-containing OPE modifications, a variance we ascribe to the different selection rules for 1PA versus 2PA transitions in a centrosymmetric complex. The extinction coefficient corresponding to λ_{max} increases on OPE bridge lengthening. While the σ_2 maximal values are found for complexes with the longest OPE bridge, there is not a clear dependence of the magnitude of σ_2 on OPE bridge length. The results from TD-DFT calculations of model complexes have provided insight into the nature of the transitions. The major deviation between experiment and theory, an experimentally perceived blue-shift in optical absorption maximum, compared to the theoretically predicted red-shift, is suggested to arise from the overlapping transitions in the spectral envelope reacting differently to thermally driven internal rotations [this is a complex issue; visually it appears that the low-lying absorption bands have multiple underlying components and shifting vibronic profiles, which further complicate the situation]. The calculations have identified the crucial frontier molecular orbitals and suggested that the dominant optical transitions are metal alkynyl to OPE π-bridge in character, with a redistribution of electron density toward the molecular center of symmetry that is largely independent of OPE bridge length.

Acknowledgment. M.G.H., M.P.C., M.S., and R.S. thank the Australian Research Council for financial support. M.G.H. is an ARC Australian Professorial Fellow.

Supporting Information Available: Full details for reference 84, syntheses of **1**−**17** and **19**−**29**, and details of the NLO and computational studies. This material is available free of charge via the Internet at http://pubs.acs.org.

(110) Cifuentes, M. P.; Powell, C. E.; Humphrey, M. G.; Heath, G. A.; Samoc, M.; Luther-Davies, B. *J. Phys. Chem. A* **2001**, *105*, 9625.
(111) Powell, C. E.; Cifuentes, M. P.; Morrall, J. P. L.; Stranger, R.; Humphrey, M. G.; Samoc, M.; Luther-Davies, B.; Heath, G. A. *J. Am. Chem. Soc.* **2003**, *125*, 602.
(112) Cifuentes, M. P.; Powell, C. E.; Morrall, J. P.; McDonagh, A. M.; Lucas, N. T.; Humphrey, M. G.; Samoc, M.; Houbrechts, S.; Asselberghs, I.; Clays, K.; Persoons, A.; Isoshima, T. *J. Am. Chem. Soc.* **2006**, *126*, 10819.
(113) Samoc, M.; Morrall, J. P.; Dalton, G. T.; Cifuentes, M. P.; Humphrey, M. G. *Angew. Chem., Int. Ed.* **2007**, *46*, 731.